Fabrication of Architectured Multilayers with Mismatched Rheological Behaviors: Layer Stability, Structure, and Confinement Dictate Polyethylene-Based Film Properties

Jixiang Li, Ibtissam Touil, Guillaume Sudre, Mohamed Yousfi, Bo Lu, Huagui Zhang, Jiabin Shen, Xavier Morelle, Abderrahim Maazouz, Khalid Lamnawar

Fabrication of architectured multilayers with mismatched rheological behaviors: layer stability, structure and confinement dictate polyethylene-based films properties

Jixiang Li [a], Ibtissam Touil [a], Guillaume Sudre [a], Mohamed Yousfi [a], Bo Lu [b], Huagui Zhang [c], Jiabin Shen [d], Xavier Morelle [a], Abderrahim Maazouz [a,e], Khalid Lamnawar [a,*]

[a] *Université de Lyon, CNRS, UMR 5223, Ingénierie des Matériaux Polymères, INSA Lyon, F-69621, Villeurbanne, France*

[b] *Key Laboratory of Materials Processing and Mold (Ministry of Education), National Engineering Research Center for Advanced Polymer Processing Technology, Zhengzhou University, Zhengzhou 450002, China*

[c] *College of Chemistry and Materials Science, Fujian Key Laboratory of Polymer Materials, Fujian Provincial Key Laboratory of Advanced Materials Oriented Chemical Engineering, Fujian Normal University, Fuzhou350007, China*

[d] *State Key Laboratory of Polymer Materials Engineering, Polymer Research Institute of Sichuan University, Sichuan Provincial Engineering Laboratory of Plastic/Rubber Complex Processing Technology, Chengdu, 610065, China*

[e] *Hassan II Academy of Science and Technology, 10100 Rabat, Morocco*

** Corresponding author. E-mail address: khalid.lamnawar@insa-lyon.fr (K. Lamnawar).*

Abstract

To better understand the processing and final properties of multilayer films obtained by layer forced assembly in co-extrusion, as well as their structure-morphology, the present study focuses on model films with LDPE as the base polymer. More specifically, the layer confinement of LDPE by a glassy amorphous polymer (here PC or PS) was investigated. First, the viscosity and elasticity ratios of the different neat polymers were measured by rheological tests to simulate the processing conditions in the feedblock and multipliers during coextrusion. These results, together with the observation of film transparency at the macroscopic scale and the layer breakup phenomena between layers at the microscopic scale enabled us to build a comprehensive stability map rationalizing the conditions required for a well-controlled multi-nanolayer architecture. Second, the morphology of the coextruded films was analyzed by SEM and TEM. The onset of the layer breakup in the LDPE/PS system was determined at 2048 layers with layer thickness of 95 nm, while in the LDPE/PC system it was at 256 layers with layer thickness of 980 nm. The layer breakup happened at fewer number of layers for LDPE/PC system due to the viscoelastic mismatched properties between the base polymers. Interestingly, we have demonstrated that it is nonetheless possible to prepare some nanolayer structures with 16380 layers of PS/LDPE system with some defects but still maintaining an overall properties improvement despite their high mismatched viscoelastic properties. Finally, the orientation and crystalline structure of the coextruded films were characterized by 2D-WAXS and DSC, and the ultimate properties of the films were determined through tensile testing. The geometrical confinement of LDPE nanolayer did not affect the thermal crystalline properties of LDPE chains, but it affected the crystalline morphologies as well as the final mechanical response of the obtained multilayers films.

Key words: Force assembly co-extrusion, Low Density Polyethyelene, Polystyrene, Polycarbonate, multilayer films, layer confinement

1. Introduction

Flexible and lightweight functional multilayer films are in a growing demand in fields of printed electronics[1], energy[2], nanomedicine[3], automotive[4] and construction industries[5]. Numerous methods were designed for combining various polymers to produce multilayered films such as layer-by-layer assembly[6], lamination[7], multilayer coextrusion[8], solvent casting[9], or spin coating[10]. Among them, forced-assembly multilayer coextrusion is becoming popular due to the significant increase in industrial demand to create and produce at large-scale new and continuous multifunctional organic materials with enhanced characteristics[11]. This layer multiplication process was initially developed by Dow 40 years ago and more recently updated by Baer's group at Case Western Reserve University[12]. It was reported that the forced-assembly multilayer coextrusion could endow films with enhanced optical properties[13, 14], mechanical properties[15], gas barrier properties[16, 17], and dielectric properties[18].

Several reviews and studies have described the process of multiplication via forced assembly[11, 12, 19]. To simplify, the two initial polymer melts are first converged in a feedblock where the A/B or A/B/A layer structure can be formed according to the structure of the feedblock. The layered flow then goes through multipliers where the layered flow is cut, spread, stretched and stacked as shown in figure 1. By changing the number of multipliers, films with several layers to thousands of layers are fabricated. It is worth noting that the uniformity and integrity of layer structures depends highly on the stability of flow inside the multipliers[11, 12, 19], in other words, the matched viscosity of the two polymer melts. Significantly mismatched viscosities of the two polymer may lead to the low viscosity layer encapsulating the high viscosity layer giving rise to layer instability[20, 21] and layer break-up[22, 23] phenomena. We have carefully studied the instable interfacial phenomenon during and after forced assembly in our previous work[24]. To obtain better uniform layer structures, efforts were made by not only matching the viscosity of the melts but also optimizing the multiplier, feedblock or extruder die design. For example, with a mismatch viscosity pair of polystyrene/poly(methylmethacrylate) (PS/PMMA) and hard/soft thermoplastic polyurethanes (TPUs), co-extruded films with up to 65 layers were successfully produced using a combination of a 9-layer feedblock, low-pressure drop multiplier dies, and external lubricants[25]. A gradual stacking channel and a longer flow path length were also proved to be beneficial for the layer thickness uniformity[11].

Among the commonly used polymer pairs for co-extrusion, LDPE and PS were regarded since the year of early 1976[26, 27]. The multilayer film properties (i.e, tensile strength and barrier) were enhanced[28]. Recently, the LDPE/PS multilayer films were reported to exhibit excellent physical and laser-marking properties[29]. The amorphous PS with higher T_g can also be regarded

as a confinement layer used to influence the crystallization of LDPE[30]. Similarly, Polycarbonate (PC) as an amorphous polymer with an even higher T_g is also able to produce layer confinement[31]. However, the highly mismatched viscoelastic properties of LDPE/PS and LDPE/PC is the critical problem which affects the layer uniformity and integrity dramatically, especially for nanolayer films. Few studies focused on detecting the processing window required for the LDPE/PS or LDPE/PC multilayer systems to fabricate well architected micro-/nano-layer films. Moreover, and despite the interesting works dedicated to forced-assembly layer coextrusion, there are very few papers dealing with the study of layer flow instabilities and how they are influencing the structure and mechanical properties of the obtained multi-micro/nanolayers[19, 32-34].

Several studies have shown that two polymers associated in a multilayer structure are capable of developing synergistic effects by modifying their deformation mechanism [28, 35, 36]. For example, by combining two materials, one fragile like polystyrene (PS), the other ductile like PE, Schrenk et al.,[28] discovered that PS, in between two layers of PE (i.e. 3 microlayers), can reach, in uniaxial tensile loading, deformation values significantly higher than those obtained when it is in a single layer, the PE layer then making it possible to block the propagation of transverse cracks formed in the PS layer. In addition, studies [35, 36] carried out on multi-microlayers of polycarbonate (PC), a tough material, and styrene-acrylonitrile copolymer (SAN), a fragile material, have shown that the mechanical behavior depends not only on the proportion of the two materials but also on the thickness of the layers of each material. Multilayers composed with a higher proportion of SAN or with thicker layers, present a rather fragile behavior resulting from the preferential activation of cavitation mechanisms in the SAN layers. On the other hand, when the proportion of PC increases or the thickness of the layers of the two materials decreases, the multilayer structures are increasingly ductile and tough. This is attributed to a change in deformation mode of SAN when it is found in a thin layer in the multilayer structure. Thus, in the case of multilayers made up mainly of PC with layers of SAN with a thickness up to one micron, cavitation mechanisms through crazing in the SAN layer are almost non-existent; they give way to shear yielding mechanisms leading to the formation of necking which propagates both in the PC and SAN layers[35, 36].

Lai et al.,[37] prepared through a forced-assembly coextruded multilayer films with 33, 257, and 1025 alternating semi-crystalline EAA (ethylene-co-acrylic acid copolymer) and PEO (poly(ethylene oxide) layers. The authors found, by reverse modelling, that the PEO modulus increased as PEO layer thickness decreased which was attributed to stress redistribution to the higher modulus aligned PEO lamellae within the layers. On the other hand, layer thickness had

not influenced the yield stress. However, a decrease in the yield strain was noticed in the case of thin layers and no yield point was detected when PEO layer thickness approached the thickness of a single lamella. This was assigned to a decrease in interlamellar spaces between PEO lamellae due to greater alignment of the crystalline fraction in the deformation direction.

In the case of fully amorphous multilayer systems, Burt et al.,[38] utilized multilayer co-extrusion to investigate the role of the interface and the effect of confinement on the mechanical properties of polystyrene-*block*-poly(ethylene-co-propylene)-*block*-polystyrene triblock copolymer (SEPS) confined between PMMA layers. In the extrusion direction (ED), PMMA/SEPS multilayer films showed an increase in elongation at break and toughness as layer thickness decreased from 800 to 100 nm which indicates a shift from brittle to ductile failure. Similar layer-thickness-dependent increase in ductility has been observed in PC/PMMA and PC/SAN multilayer films[13]. However, the elastic modulus and yield stress decreased with decreasing layer thickness.

The present work successfully defined a processing window to fabricate stable flow, well-architectured and continuous multilayer films with rheologically mismatched LDPE / (PS or PC) systems. A better understanding of the effect of confinement on the structural and morphological properties was also obtained. The crystalline morphology as well as micro-/nano-structuration of the obtained multilayers were characterized through wide angle X-ray scattering (WAXS) and electron microscopy (SEM, TEM). In addition, tensile tests eventually assessed the impact of such confinement on the ultimate mechanical properties of the fabricated films. These characterizations helped us not only to quantify the level of confinement obtained in the different multi-layered systems (with a number of layers going from 2 to 16380) but also to stress the importance of stable layer microstructure to ensure a beneficial effect on properties of such confinement. Herein, 16340 L is a critical reference system to deeply investigate the crossed influence of effective confinement and unstable flow micro/nanolayer structures.

2. Experimental section

2.1 Materials and sample preparation

The polymers investigated in this study are as follows: low-density polyethylene (LDPE), polystyrene (PS), and polycarbonate (PC). The main characteristics of these materials are listed in Table 1. Weight average molecular weight (M_w) and polydispersity index Đ were determined by high-temperature steric exlusion chromatography at 150°C using 1,2,4-trichlorobenzene as the eluent for LDPE and tetrahydrofuran (THF) for PS and PC. The activation energy of the

viscous flow (E_a) was determined from an Arrhenius law by plotting $\log\eta_0$ versus $1/T$ within a temperature range of 160°C<T<240°C.

Table 1. Characteristics of the investigated polymers.

Sample	Manufacturer	M_w (kg/mol)	Đ	η_0	E_a [kJ/mol]	ρ (g/cm^3)
LDPE	ExxonMobil 165	238	9	38459	53.5	0.92
PS	Styron 637	448	3	5429	133	1.05
PC	Calibre 303EP	22	2.5	111831	152	1.20

Multilayer structures of micro/nanolayers were produced using a homemade multilayer coextrusion setup as schemed in Figure 1. Two extruders were combined through a feedblock from where a series of layer multiplication dies were connected. The two different polymer melts first meet in the feedblock in a bilayer configuration, then, when going through the layer multiplication dies, the melt is successively split vertically and horizontally spread back to its original width before being stacked again, keeping the total film thickness constant. The final number of layers is determined by the number of multipliers used. During the coextrusion process, the melt temperature was set at 240°C for the extruders, multipliers, and die. The chill-roll temperature was set to 60°C with a drawing speed of 1.27 *m/min* used to obtain a total film thickness of 200±50 μm. The stretching ratio was kept low as the focus is mainly set on the structuration due to the coextrusion and layer multiplication processes rather than chain orientation by drawing. The feedblock configuration used for the systems was a A/B configuration, where A and B correspond to the extruders displayed in Figure 1. A set of n multipliers leads to a final film of $2x2^n$ layers, since a two-layered feedblock was used for the LDPE/ (PS or PC) systems. For clarity purpose of the present paper, only results with films based on 1:1 volume ratio will be shown and discussed.

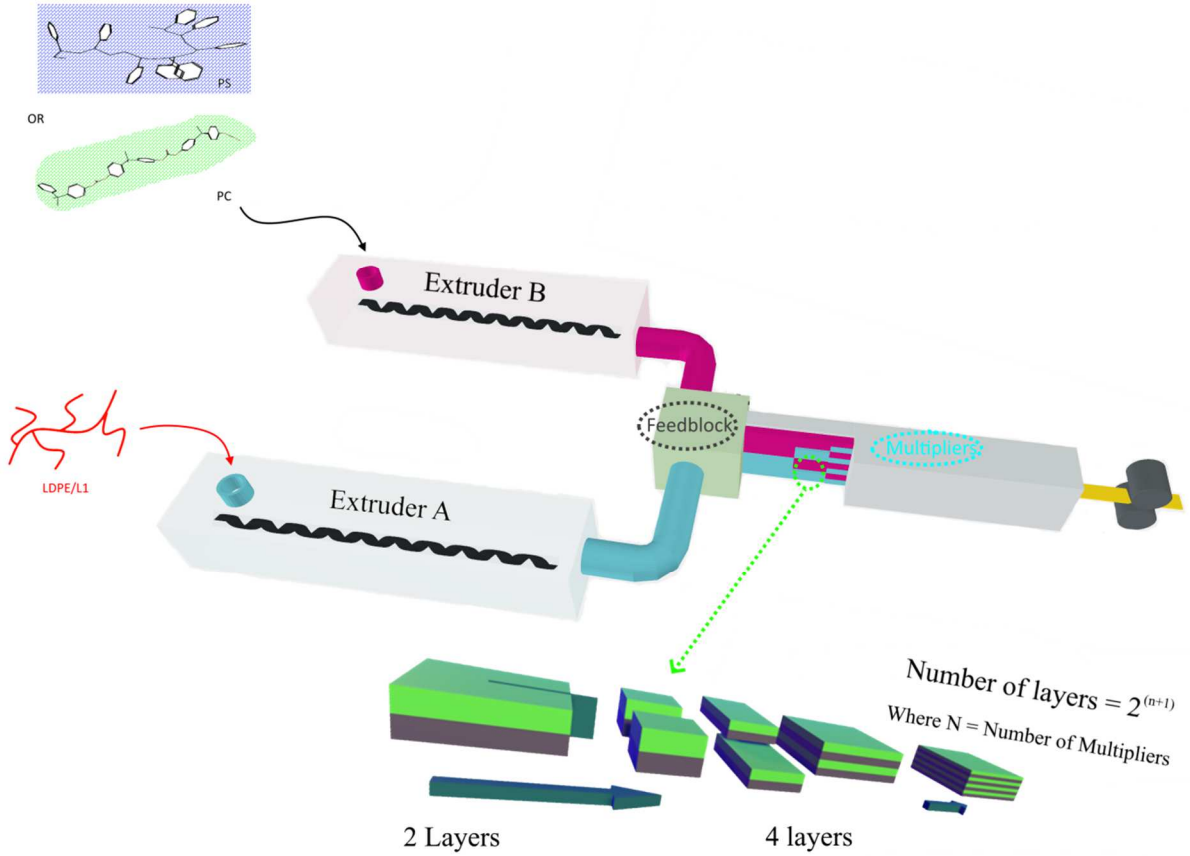

Figure 1. Schematic illustration of layer multiplication in the home-made multilayer coextrusion setup.

All produced and studied multilayer films are listed in Table 2 with LDPE combined with PC or PS, where *n* is the number of multipliers and *N* the corresponding number of layers. The estimated nominal layer thickness for each layer with a A/B film configuration was calculated using Equation 1.

$$h_{nomA,B} = \varphi_{A,B} \frac{h_{total}}{2^n} \quad (1)$$

where φ_A and φ_B represent the volume fraction of A and B, respectively, h_{total} the total film thickness and *n* the number of multipliers.

Table 2. Characteristics of the multilayered LDPE/PS and LDPE/PC films, where the h_T represent the total thickness of the film and h_N represent the thersitical layer thickness.

Polymer systems		LDPE/PS		LDPE/PC	
no. of layers (*N*)	no. of multipliers (*n*)	h_T (µm)	h_N	h_T (µm)	h_N

32L	4	160	5 μm	200	6 μm
256L	7	175	690 nm	250	980 nm
1024L	9	200	195 nm	200	195 nm
2048L	10	195	95 nm	170	83 nm
16380L	13	200	12 nm	200	12 nm

2.2 Characterization

2.2.1 Melt shear rheology

Rheological measurements of the neat polymers were performed by a stress-controlled DHR-2 (Discovery Hybrid Rheometer, TA Instruments), using 25 mm parallel-plate geometry with a gap of 1 mm. The disks of neat polymers for rheological measurements were compression-molded at 200 °C for 5 min with a pressure of 200 bars between two Teflon films to obtain a smooth surface. A dynamic frequency sweep test was done with frequencies ranging from 628 to 0.01 rad/s at fixed strain amplitude of 5% from 150 to 250°C.

2.2.2 Scanning electron microscopy **(SEM)**

The morphology of the multilayered films was observed by scanning electron microscopy (SEM) using an FEI QUANTA 250 FEG microscope in high-vacuum mode. The samples were stained by ruthenium tetraoxide vapor (RuO_4) for two days and then placed between two epoxy resin plates until consolidation. The samples were sectioned normal to the extrusion direction via a cryo-ultramicrotome (LEICA EM UC7) at room temperature using a diamond knife.

2.2.3 Transmission electron microscopy (TEM)

The morphology of the multilayer films was also characterized by transmission electron microscope (Philips CM 120) operating at an accelerating voltage of 80 kV. Extremely thin sections of about 80 nm were microtomed from specimens perpendicular to the extrusion direction using an ultramicrotome.

2.2.4 X-ray diffraction

An Oxford Diffraction Gemini A Ultra diffractometer equipped with a molybdenum (Mo) source, as well as a high-intensity, Enhance Ultra Cu X-ray (Cu K) source was used to analyze

the crystal morphology of the obtained multilayered films. These measurements were carried out at the "Henri Longchambon" diffractometry center in Lyon. A small portion of multilayer films was examined in all three orientations after being placed on a sample holder (perpendicular, transverse, and in the direction of the flow). The diffractometers were equipped with a CCD camera and controlled by CrysAlisPro software. The measurements were performed under a continuous nitrogen flow and at room temperature.

2.2.5 Tensile tests

Tensile tests were conducted on a Instron 3384 testing machine (Instron Co., UK). Dogbone specimens were cut from the coextruded films with their longitudinal direction in the direction of extrusion. The specimens' dimensions in gauge section were close to: a length L_0 of 25 mm, a width W_0 of 4 mm and a thickness th_0 around 150-200 µm. Tensile tests were performed on a MTS double column testing machine with a 100N load cell, at room temperature and a constant crosshead displacement rate of 5 mm/min (~0.0033s^{-1}). A minimum of three specimens were used for all test conditions.

3. Results and discussion

3.1 Viscosity and elasticity ratios of the studied model pair systems

Viscosity and elasticity ratios of the viscoelasticity mismatched systems were obtained using small-amplitude oscillatory shear measurements at a processing temperature of 240°C. This latter point is critical for understanding the flow behavior and the stress relaxation process during coextrusion, as well as determining the layer uniformity of the multilayer structure. The viscosity ratio and elasticity ratio are respectively defined by $M\eta^* = {\eta^*_{LDPE}}/{\eta^*_{PC\ or\ PS}}$ and $M\lambda = {\lambda_{LDPE}}/{\lambda_{PC\ or\ PS}}$ with $\lambda = G'/\omega G''$. In Figure 2, the hatched rectangle in grey represents the range of shear-rates occurring in the feedblock and in the hanger die (1–100 s^{-1})[39] and the green hatched zone indicates the shear-rate range taking place within the multipliers (1–10 s^{-1})[40]. The viscosity ratio of LDPE/PS is quite high and can reach a value of 4 at 1 s^{-1} and a value of 2 at 10 s^{-1}, while the viscosity ratio for the LDPE/PC system has a value of 2 at 1 s^{-1} and a value of 0.6 at 10 s^{-1}. It is interesting to note that the LDPE /PC system has, in contrast, an elasticity ratio at least three times higher than that of LDPE/PS in the shear-rate range taking place in the multipliers. These values are also summarized in

Table 3.

Table 3. Values of viscosity ratios and elasticity ratios of the studied polymer couples.

	Viscosity ratios M_{η^*}	Elasticity ratios M_λ

Shear rates (s^{-1}) assuming Cox-Merz rule	LDPE/PS	LDPE/PC	LDPE/PS	LDPE/PC
1	4.0	2.0	7.2	49
10	2	0.6	3	9
100	1.0	0.3	1.3	3

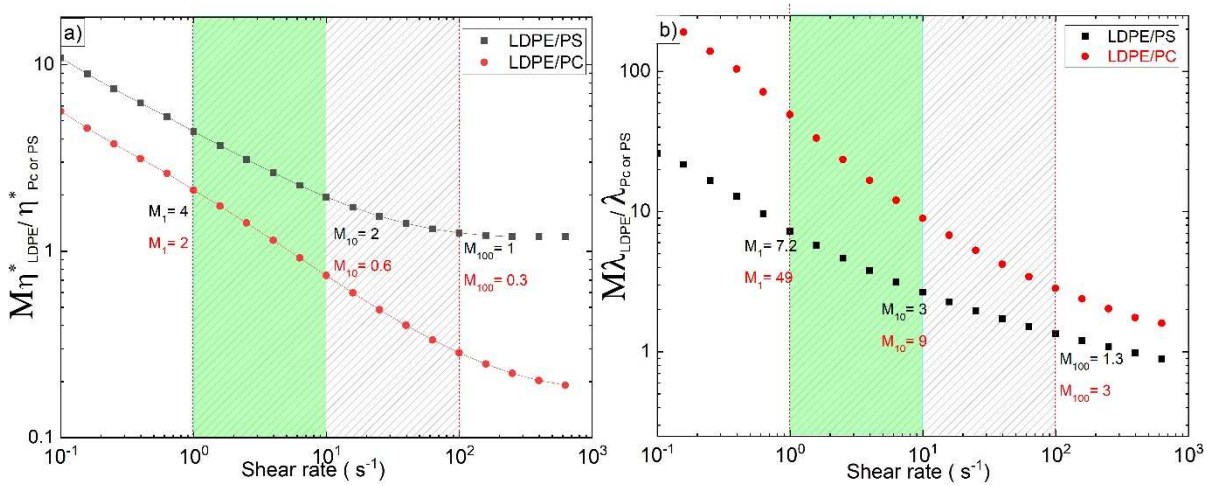

Figure 2 Viscosity ratio (a) and elasticity ratio (b) versus the flow rate for immiscible systems: LDPE /PS (black curve), and LDPE /PC (red curve).

3.2 Estimation of contact time and nominal thickness in multilayer coextrusion with various numbers of layers (N)

Quantifying the contact time between neighboring layers is required to characterize the polymer-polymer adhesion[8]. The contact time should not be too long to keep the interface stable throughout the coextrusion process. The contact time is defined as the period required for the polymer to flow sequentially through the confluent zone of the manifold system, the series of multipliers (LME), and the die. In this study, the contact time for all multilayered films is determined as a function of the number of multipliers (n) as follows[41]:

$$t_{cont} = \frac{V_{conf} + nV_{LME} + V_{die}}{Q_{mass}}\rho$$

where V_{conf}, V_{LME}, and V_{die} denote the volume of the confluent area in the feed-block, in one-layer multiplying element, and in the die, respectively; and n represents the number of multipliers used. Q_{mass} refers to the mass flow rate and ρ denotes the apparent density of confluent melts at the extrusion temperature. The corresponding values are summarized in Table 4. The estimated contact time and the theoretical layer thickness h_N for LDPE /PC and LDPE /PS are plotted in Figure 3 as a function of the number of layers N (or alternatively of the number of multipliers n). It is noticeable that the contact time of these multilayered

structures increased with the number of layers, or alternatively with the number of multipliers, logically accompanied by a decrease in nominal layer thickness. This was as expected, since each time that layers are multiplied through coextrusion, a new interface is produced, resulting in a longer melt contact time and a thinner layer down to several nanometers for the nanolayered structures[8].

Table 4 Values of the confluent area in the feed-block, one-layer multiplying element, die and volume flow

$V_{conf}\ (cm^3)$	$V_{LME}\ (cm^3)$	$V_{die}\ (cm^3)$	$Q_v\ (cm^3/s)$
1.95	7.75	43.89	26.6

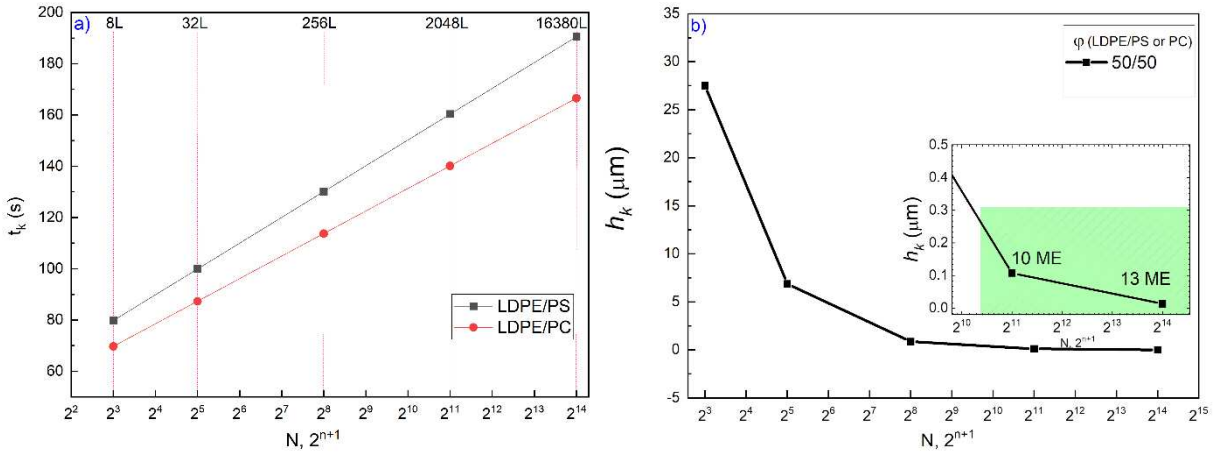

Figure 3 contact time (a) and theoretical thickness (b), for immiscible multilayer films with various numbers of layers (N) or the number of multipliers (n) ($N=2^n+1$). ME means multiplier element.

3.3 Architecture and morphology of coextruded multi-micro/nanolayers

3.3.1 Multilayer stability map

A Stability map for all coextruded films with stable and unstable domains was constructed (see Figure 4). The appearance of the films is shown schematically according to the ratio of viscosity against volumetric flows of 50/50 at 240°C. For the immiscible LDPE /PS pair, the viscosity and elasticity ratio are between 2 and 3 at 10 s^{-1} (Table 3). The resulting films appeared to be stable, especially for a number of microlayers going from 32 layers to 1024 layers. In contrast, as we increased the number of layers up to 2046, defects appeared in the films which are mainly caused by unstable flows illustrated by the unstable pictures in the inset of Figure 4. When the number of layers reached 16380, more instability phenomenon can be observed along

with some heavy waves appeared as shown by the waves pictures in Figure 4. For the LDPE/PC system with a viscosity ratio of 0.6 and an elasticity ratio around 9 at 10 s^{-1}, the films obtained seemed to be relatively stable for a number of micrometric layers lower than 256. As the number of layers increased to 1024 and 2048, severe instabilities including unstable and waves shown in Figure 4 were observed, along with somewhat chaotic interfacial defects. The encapsulation at the edge (Figure 4) of the films was also observed when the number of layers increased to 16380. The reason for these unstable phenomena was mostly the viscosity mismatch of LDPE and PS/PC which caused the flow instability during forced assembly.

To conclude, the LDPE /PS system was more stable than the LDPE /PC system. This is possibly due to the lower elasticity ratio of LDPE /PS than that of LDPE/PC, which may improve the interfacial stability of coextrusion. It is important to note that in both immiscible systems (LDPE /PS and LDPE /PC), delamination was only observed for a low number of layers (i.e multi-microlayers) because of insufficient adhesion between the layers.

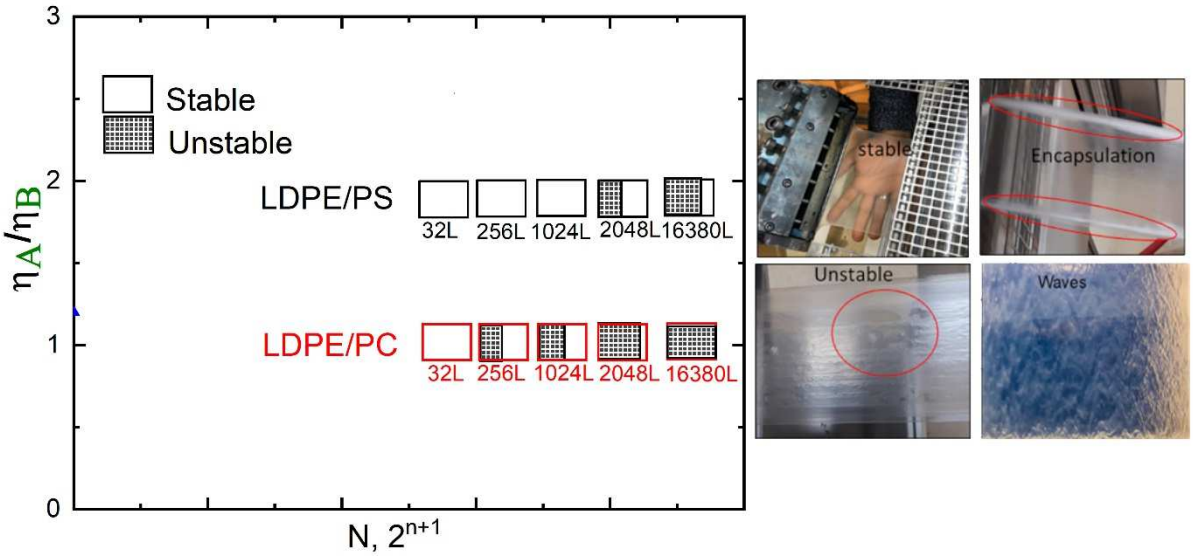

Figure 4 Chart of stability/instability observed experimentally for different couples of coextruded films with the plot of viscosity ratios at 10 s^{-1} versus numbers of layers (N) or the number of multipliers (n) ($N=2^{n+1}$) using a reference temperature of 240°C (A= LDPE; B= PS or PC).

3.3.2 Layer architecture/structure

Figure 5 and Figure 6 show SEM micrographs of the multilayer LDPE /PS and LDPE /PC immiscible systems respectively, for an identical total thickness of 200 µm. Here, the LDPE layers are light grey, and the PC and the PS appear in a darker shade. This good contrast is due to the use of different staining between LDPE, PC, and PS by using ruthenium tetroxide (RuO_4),

which can improve the visualization of the internal structure. Depending on the studied system, the multilayer films can form a continuous, uniform layered structure. As imaged by SEM (see Figure 5 (a-c)), uniform and continuous LDPE and PS layers are clearly observed, with sharp interfaces and continuous structure for films ranging from 32 to 1024 layers. However, as the layer thickness decreases from microscale to nanoscale, some layers remain continuous and some layers begin, in places, to break up into nanosheets and nanodroplets (i.e., 2048L, Figure 5 (d)). The onset of the breakup layer in the LDPE/PS system was determined at 2048 layers with a theoretical nominal thickness h_N of 95 *nm* (

Table 2), which is around the gyration radius of the studied polymers. In Figure 6 (a), for the micro-layered 32L film, it can be seen that LDPE and PC layers are clearly distinguished and continuous, even though the thickness of the layers is noticeably irregular. Note that for both systems, the layer thickness measured significantly differs from the theoretical layer thickness (Table 2) being overall larger than expected which can be partly explained by a non-fully uniform flow distribution through the width of the film materialized by the presence of edge defects (see inset in Figure 4) and differences of thickness between the center and the edges of the film. For LDPE/PC system, when the number of layers is increased to 256L (h_N = 980 *nm* – Figure 6 (b)), the film is divided into two areas, one with continuous layers and the other with break-up layers and nanodroplets. It is also worth noting that in the 2048L and 16380L LDPE/PC films, the layers of LDPE and PC can no longer be distinguished. Mismatch in viscoelastic properties between the polymers may be the reason for the nonuniformity across the layers[12].

Despite PS and LDPE not being matched in viscoelastic properties, the LDPE/PS layered systems prepared by forced-assembly coextrusion display stable and continuous interfacial properties probably thanks to their relatively low elasticity ratio mismatch (i.e.,3). In contrast, having a higher elasticity ratio of 9, the LDPE/PC films have more defects than the LDPE /PS and much earlier layer breakup threshold.

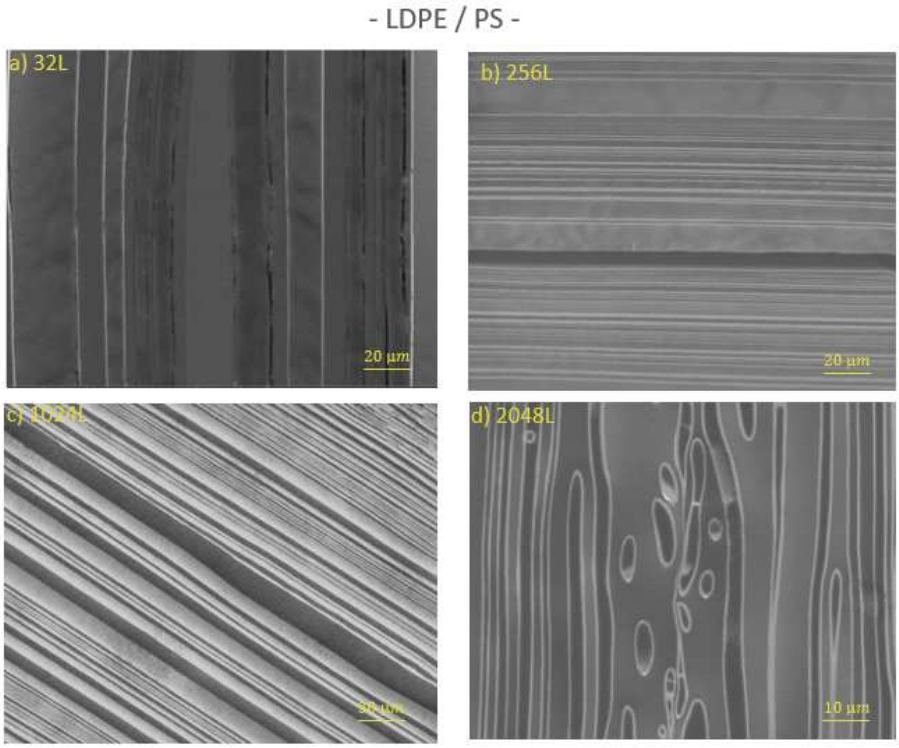

Figure 5 SEM micrographs of the multilayer LDPE/PS system ranging from 32L to 2048L. LDPE is in light grey while PS is in darker grey.

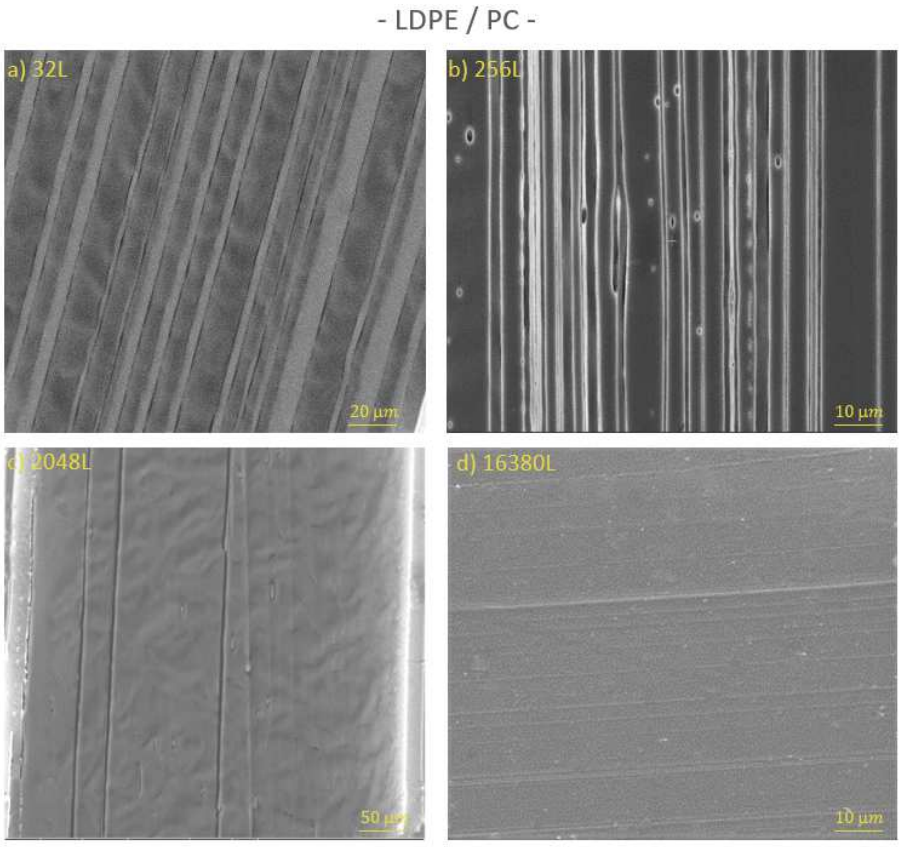

Figure 6 SEM micrographs of the multilayer LDPE /PC system ranging from 32L to 16380L. LDPE is in light grey while PC is in darker grey.

Figure 7 shows the nanometric morphology of LDPE/PS nanolayered films with layers numbers of 2048L (a-e) and 16380L (f and g) by TEM. In coherence with previous SEM images, these multilayered films are mostly continuous, with more or less uniform thickness outside of the defect regions having interfacial distortions such as layer breakup and nanodroplet formation (Figure 7 (a)). We can also see that the interface between LDPE and PS is visibly sharp (i.e., no diffuse interphase). Moreover, these micrographs reveal that for the LDPE /PS system, lamellar morphologies are still observed in films with a high number of layers (i.e., ≥2048-layers). Hereto, we have demonstrated that it is possible to prepare some nanolayer structures with 16380-PS/LDPE systems despite their high mismatched properties. It has also been demonstrated that lower elastic contrast is a key to stabilize their flow structure in nanolayered systems. LDPE crystals appear as bright stripes and tend to be organized into flattened spherulites (2D) (see Figure 7 (e) and (g)). Indeed, in the 2048-L film and in films with above layer number, LDPE layers thickness are significantly smaller than the typical dimensions of bulk LDPE spherulites (100 µm)[42]. It is thus assumed that as the number of layers increases, the spherulites transform from 3D spherulites to somewhat compressed 2D spherulites, or even to strongly oriented lamellae arranged unidirectionally (1D) in the extrusion direction. This hypothesis will be investigated in the next section by analyzing the crystalline structure of LDPE.

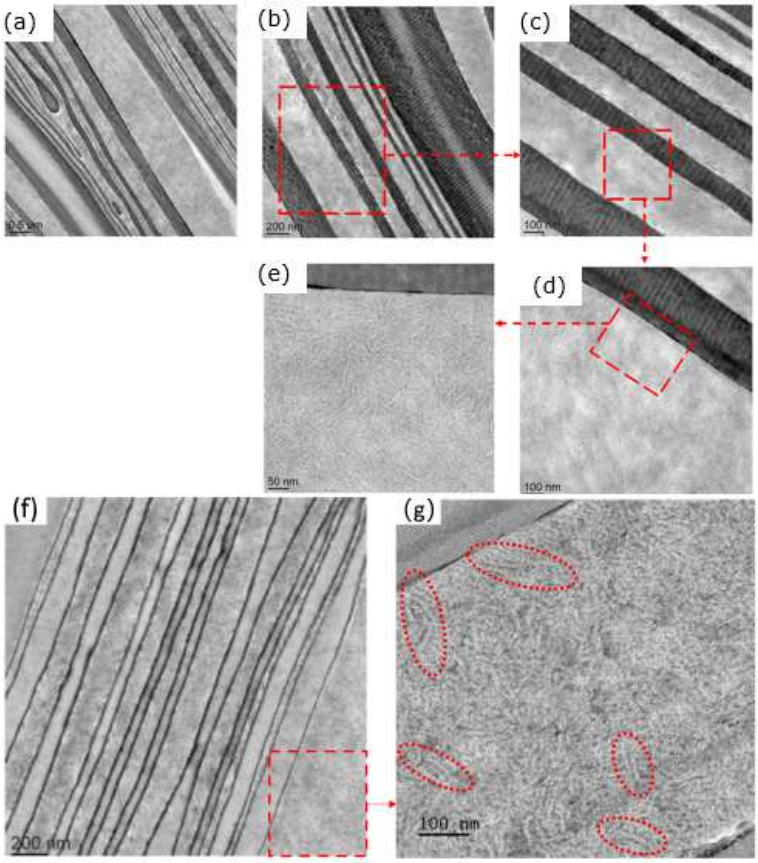

Figure 7 TEM micrographs of 2048 LDPE/PS (a-e) multilayered structures and16380 LDPE /PS (f and g) multilayered structures. Crystalline and homogeneous structure is highlighted from (f) to (g).

3.4 Crystalline structure

The orientation and crystalline structure of LDPE in multilayered LDPE/(PS and PC) films as well as in a reference neat LDPE film were characterized by 2D-WAXS patterns with an X-ray incident beam in the extruded (ED) and normal (ND) directions to the film plane (see Figure 8 (a)-(h)).

The LDPE control specimen exhibits two isotropic rings (Figure 8 (e)). The first ring at (2θ =21.33°) and the second ring at (2θ =23.66°), corresponding to (110) and (200) planes in the orthorhombic crystal structure of polyethylene[43], imply that the LDPE lamellae are randomly oriented (i.e. in an isotropic fashion) in the extruded monolayer film. Figure 8 (i) and (j) depict the 1D profiles for coextruded LDPE/PS, and LDPE/PC multilayers, respectively. In all prepared multilayer films, the peaks from the (110) and (200) planes are visible in the 1D profile superposed with the wide amorphous halo of PS (Figure 8 (i)) or PC (Figure 8 (j)), respectively.

For LDPE/PS systems, it can be seen from Figure 8 a-d, that the (110) plane appears as an isotropic ring in the ED direction for all multilayers, suggesting no significant anisotropy in LDPE chains orientation. Nonetheless, for the 16380 layered films (Figure 8 (d)), a strong equatorial concentration of the (200) plane was observed in the ED direction. This orientation can be attributed to the geometric confinement (at the nanoscale) caused by the glassy PS on the LDPE during the cooling of multilayers. It is assumed that by increasing the number of layers from 32 to 16380L or decreasing the individual theoretical LDPE layer thickness from $5\mu m$ to $12nm$, the LDPE spherulites transform from 3D to flattened (2D) spherulites, and then to stacked in-plane lamellae[30]. This finding complies with the TEM results (Figure 7 (e) and (g)).

However, for the case of coextruded LDPE/PC films an amorphous halo with no distinctive scattering concentration zone is shown in Figure 8 (f-h). The peaks of (110) and (200) planes for LDPE are still evident in the 1D profile superposed with the wide amorphous halo of PC, confirming the presence of the crystal structure of LDPE. The rigid PC segments (T_g=150°C) strongly reduces the molecular mobility of LDPE segments during crystallization and consequently reduce the crystallization process of LDPE, resulting in a less crystallized film. This observation will be further verified by DSC measurements showing a smaller value of crystallinity for LDPE/PC multilayers.

The DSC thermographs of heating scans for LDPE /PS and LDPE /PC multilayers and their blend are shown in Figure 9 (k) and (l) respectively, with a constant weight fraction of 50/50. The corresponding values of DSC measurements are summarized in Table 5. We can note negligible changes in terms of melting temperature, crystallinity ratio and lamellar thickness (the latter obtained by SAXS) between the different coextruded films of a given system as well as their corresponding reference blend. Additionally, we note that the crystallinity of the coextruded LDPE/PC films is very low around 1%, confirming the more pronounced amorphous behavior observed in WAXS.

To conclude, the gathered results suggest that the geometrical confinement from micro to nanolayer did not affect the thermal crystalline properties of LDPE systems, but rather only their morphology as demonstrated by WAXS, TEM, and SEM.

Table 5 DSC parameters for a) LDPE /PS and b) LDPE /PC multilayers, blend (50/50), and neat LDPE

	A) LDPE /PS				B) LDPE /PC			
	T_m (°C)	ΔH_m (J/g)	$X_{c,\,DSC}$ (%)	L_c (nm)	T_m (°C)	ΔH_m (J/g)	$X_{c,\,DSC}$ (%)	L_c (nm)
LDPE	112	117	40	9.47	112	117	40	9.47
32L	110.5	24.5	16.9	9.01	110.7	0.8	0.5	9.4
256L	111.7	29.7	21	9.38	109.7	1.4	1.1	9
2048L	110.6	30.8	21.3	9.04	109.9	2.2	1.4	9.47
16380L	109.8	26.5	18.3	8.81	109.2	4.4	3.1	9
Blend	113	25	17.3	9.81	110.7	0.9	0.61	-

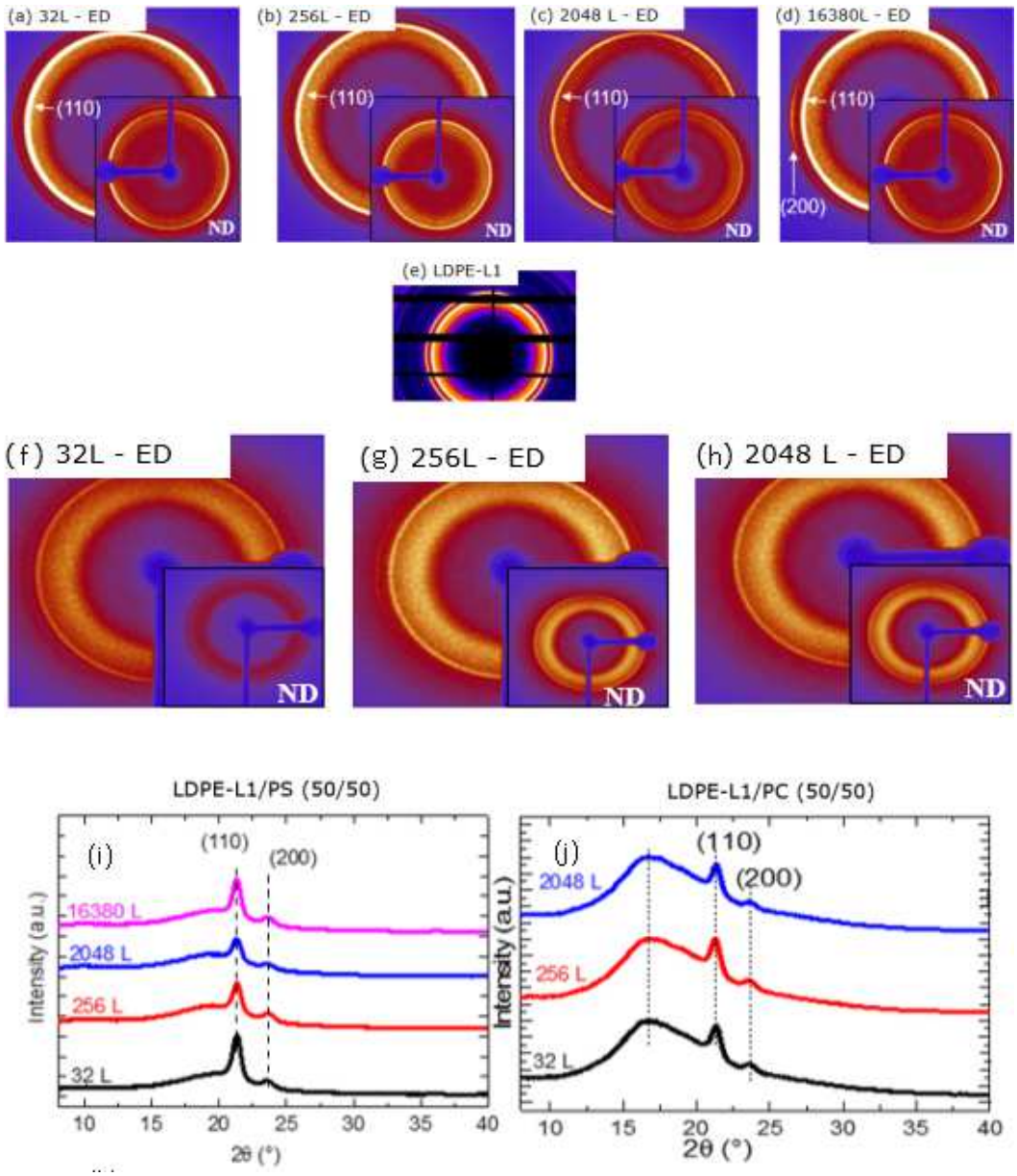

Figure 8 2D-WAXS profiles recorded with an X-ray beam in the extruded (ED) and normal directions to the film plane for the neat LDPE (reference - e), for LDPE/PS (a-d) and for LDPE/PC (f-h) multilayers films with different number of layers; 1D-WAXS profiles for coextruded LDPE/PS (i) and LDPE/PC (j) multilayers where the intensity was normalized

with the thickness of the studied films. The scattering angle is denoted as 2θ;

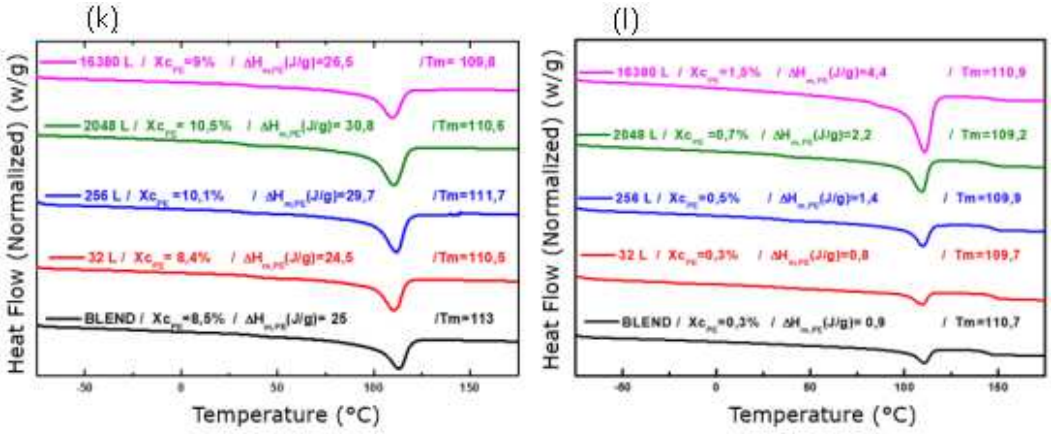

Figure 9 DSC thermographs of heating scan for co-extruded LDPE /PS (k) and LDPE /PC (l) multilayers systems and blend (all with a 50/50 weight fraction).

3.5 Mechanical response in tension

In this section, we study the mechanical response of the different coextruded films tested under uniaxial tension. We choose to focus here only on the LDPE/PS system, as it has a larger panel of stable multilayers films, and thus the combined effect of confinement (by increasing the number of layers or alternatively decreasing each layer thickness) and layer stability on the mechanical response of the films can be more thoroughly investigated.

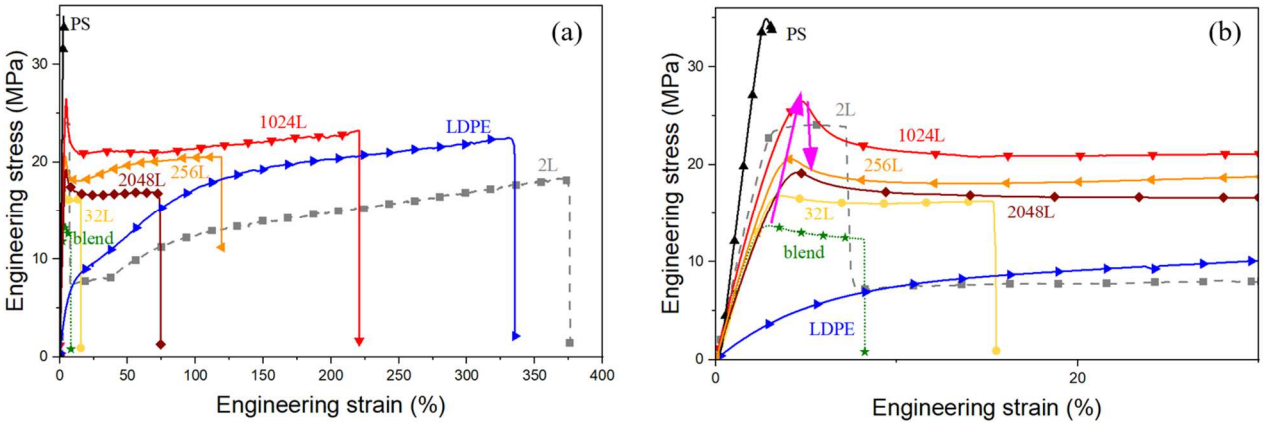

Figure 10 (a) Engineering stress - engineering strain curves under uniaxial tension for the LDPE and PS reference materials as well as for a series of multilayered films (with 50/50 weight ratio of LDPE and PS) fabricated by forced assembly coextrusion and their corresponding blend. The number of layers in the composite films is varied from 2 (microlayered films) up to 2048 layers (nanostructured films). (b) Zoom on the small strain/yield region of the curves. Magenta arrows illustrate the optimum in mechanical response obtained for the most confined multilayer without layer break-up phenomena, the 1024L films.

Figure 10 shows the engineering stress-strain curves for the different multilayers films obtained with the LDPE/ PS system (from the bilayer up to 2048 layers), as well as the reference

curves for the base polymers PS and LDPE and the corresponding blend. As expected, while glassy PS (black curve with upward trianglesymbol) is rigid and breaks at small strains (~3-4%) but with the highest stress at break (barely passing its yield stress), semicrystalline LDPE (blue curve with right direction triangle symbol) has the lowest Young's modulus and is able to deform up to very large strains (~350%) but at a more average stress level. These two base materials are good examples of the typical mechanical response paradigm in materials science between soft/ductile materials and rigid/brittle ones. By fabricating multilayer films through forced assembly coextrusion, we obtain a composite behavior in between these two extreme responses. However, if the blend specimen illustrates the usual trade-off (i.e. low strength and small ductility) between PS and LDPE response, increasing layer confinement from micro- to nano-layered systems enables to progressively reach properties closer to the best of the two worlds, ensuring both high stress and large strain at break. Moreover, one can see that the best mechanical properties are obtained with the 1024L films which correspond to the highest level of confinement without layer stability defects (which are expected to have a direct impact on the mechanical response, especially regarding fracture initiation). Similar conclusions can be drawn for the LDPE/PC system which is illustrated in Figure S3 in supplementary. We hypothesize that this synergy effect might be due to several contributions : (i) on one side, as demonstrated in the previous section and in other works[30], confinement of LDPE by glassy PS leads to a change of crystalline morphology (towards oriented stacked in-plane lamellae) that could boost the mechanical response in the extruded direction ; (ii) on the other side, increasing the number of layers tends to increase the contribution of interface/interphase regions which could improve the composite response (through better stress transfer or alternatively dissipative mechanisms such as partial debonding); (iii) and eventually the presence of multiple layers of brittle PS sandwiched between ductile LDPE layers, might also help stabilizing potential cracks and early fracture of PS, as for the tri-layers of Schrenk et al.[28].

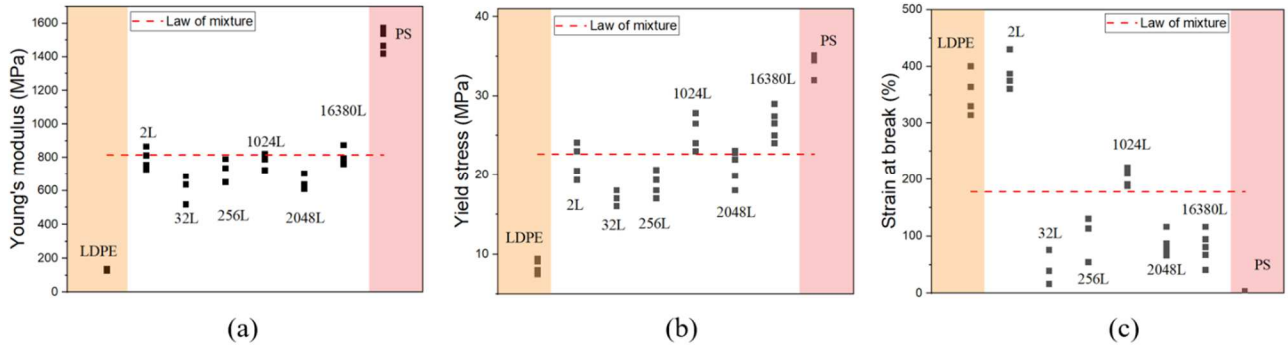

Figure 11 (a) Engineering stress - engineering strain curves under uniaxial tension for the LDPE and PS reference materials as well as for a series of multilayered films (with 50/50 weigth ratio of LDPE and PS) fabricated by forced assembly coextrusion. The number of

layers in the composite films is varied from 2 (microlayered films) up to 1024 layers (nanostructured films). (b) Zoom on the small strains/yield region of the curves.

The more specific case of the bilayer of LDPE/ PS partly supports this latter statement. Indeed, the response of the bilayer (gray dashed square curve) is first governed by the rigid response of the PS until it yields and break (visible during the test as shown in Figure S2 in supplementary and by the marked stress drop on Figure 10(b)), while the second part of the response simply corresponds to the LDPE response (showing half of the stress of the reference LDPE, as the thickness of the partly ruptured bilayer is now half of its initial thickness). Moreover, we can clearly see in Figure 10 (b) that the PS in the bilayer is able to deform significantly more (7.5% - twice more) than its reference counterpart. For all the other multilayer films, no sequential fracture of PS vs LDPE can be clearly observed and all films uniformly deform until failure of the specimen.

To conclude, Figure 11 summarizes the effect of increasing the layer number on the main mechanical properties respectively: (a) Young's modulus, (b) yield stress, and (c) strain at break. If the elastic response (i.e., Young's modulus) closely follows the law of mixture (red dashed line corresponding to 50/50 weight fraction) between PS and LDPE for all multilayers, we more clearly see the improvement brought by the nanolayered confinement in the plastic and fracture regime. Indeed, in contrast with prior studies[37,38], here, the multilayer yield stress progressively increases while layer thickness decreases, up to an optimum corresponding to the 1024L film after which the trend is less clear probably due to layer stability break-up phenomena. Interestingly, 1024L films are able to not only outperform other multilayers but also surpass this law of mixture (Figure 11 (b)). For the strain at break, exception made from the 2L which corresponds mainly to the LDPE response, 1024L films once again outperform all other multilayers. It worth noting that despite not being as good as 1024L, multilayered films with higher confinement but containing layer stability defects (such as 2048L or 16380L) still perform rather well, confirming that mechanical improvement brought by higher confinement can somewhat partly compensate for layer stability breakup. These observations are also confirmed for the case of LDPE/PC system where the best mechanical response is obtained for 256L films but where films with higher confinement (i.e., number of layers) perform almost as well if not slightly better for some properties (e.g., yield stress) as shown in Figure S3 in the SI. To conclude, if the present work confirms, in agreement with studies on other multilayer systems in the literature[13,35-38], that confinement helps improving the overall mechanical response of the obtained multilayers, this beneficial effect is only possible when layer stability is accounted for, therefore stressing the need of a good criterion to predict the layer stability.

4. Conclusion

In summary, we fabricated a series of well-architectured multilayer polymer films composed of LDPE, PS and PC. From the build-up of stability maps for all coextruded films defining stable and unstable domains, we found that LDPE/PS system is more stable than LDPE/PC system. This is assumed to be due to the lower elasticity mismatch ratio of LDPE/PS compared to that of LDPE/PC, which may improve the interfacial stability during the coextrusion process. Owing to the high mismatch in their viscoelastic properties and their immiscibility, the layer breakup increased dramatically when the layer thickness reached nanometric scale. Nonetheless, despite the presence of some layer stability defects, we have demonstrated that it is still possible to prepare some nanolayered structures with up to 16380 layers for LDPE/PS systems with relatively good properties (optical transparency and mechanical response). In addition, we highlighted through TEM images and WAXS measurements that the confinement effect of glassy PS on LDPE chains gives rise to a stacked in-plane lamellae crystalline morphology. We found that the geometrical confinement from the nanolayers did not affect the macroscopic thermal crystalline properties of LDPE chains, but mostly affected the crystalline morphologies. Meanwhile, confinement brought by increasing the number of layers enabled to enhance the mechanical response of the obtained composite by combining both the ductility of the LDPE and the stiffness and strength of glassy PS or PC. Above all, our work highlighted the great potential of forced assembly coextrusion (combined with multiplication dies) to prepare highly structured polymer multilayer systems with improved properties based on immiscible polymer pairs despite their mismatched viscoelastic properties, as long as their elasticity ratio mismatch is not too strong.

The present work was partly based on the PhD thesis entitled *"Multi-micro/nanolayers of highly mismatched viscoelastic polymers based on polyethylene with varying macromolecular architectures: Multiscale investigations towards better control of their structuration and recycling by coextrusion", Ibtissam Touil,* HAL Id: tel-03738150, version 1.

Supporting information

Thermal properties information of LDPE, PS and PC, mechanical properties of LDPE/PC systems and transparency of the multilayer films.

References

(1) Bollström, R.; Määttänen, A.; Tobjörk, D.; Ihalainen, P.; Kaihovirta, N.; Österbacka, R.; Peltonen, J.; Toivakka, M. A multilayer coated fiber-based substrate suitable for printed functionality. *Organic Electronics* **2009**, *10*, 1020-1023.
(2) Qian, J.; Han, Y.; Yang, C.; Lv, P.; Zhang, X.; Feng, C.; Lin, X.; Huang, S.; Cheng, X.; Cheng, Z. Energy storage performance of flexible NKBT/NKBT-ST multilayer film capacitor by interface engineering. *Nano Energy* **2020**, *74*, 104862.
(3) Yu, X.; Liao, X.; Chen, H. Antibiotic-loaded MMT/PLL-based coating on the surface of endosseous implants to suppress bacterial infections. *International journal of nanomedicine* **2021**, *16*, 2983-2994.
(4) Guadagno, L.; Vertuccio, L.; Foglia, F.; Raimondo, M.; Barra, G.; Sorrentino, A.; Pantani, R.; Calabrese, E. Flexible eco-friendly multilayer film heaters. *Composites Part B: Engineering* **2021**, *224*, 109208.
(5) Zhang, X.; Xu, Y.; Zhang, X.; Wu, H.; Shen, J.; Chen, R.; Xiong, Y.; Li, J.; Guo, S. Progress on the layer-by-layer assembly of multilayered polymer composites: Strategy, structural control and applications. *Progress in Polymer Science* **2019**, *89*, 76-107.
(6) Lipton, J.; Weng, G.-M.; Röhr, J. A.; Wang, H.; Taylor, A. D. Layer-by-layer assembly of two-dimensional materials: meticulous control on the nanoscale. *Matter* **2020**, *2*, 1148-1165.
(7) Anukiruthika, T.; Sethupathy, P.; Wilson, A.; Kashampur, K.; Moses, J. A.; Anandharamakrishnan, C. Multilayer packaging: Advances in preparation techniques and emerging food applications. *Comprehensive Reviews in Food Science and Food Safety* **2020**, *19*, 1156-1186.
(8) Lu, B.; Lamnawar, K.; Maazouz, A.; Sudre, G. Critical role of interfacial diffusion and diffuse interphases formed in multi-micro-/nanolayered polymer films based on poly (vinylidene fluoride) and poly (methyl methacrylate). *ACS applied materials & interfaces* **2018**, *10*, 29019-29037.
(9) Bastante, C. C.; Silva, N. H.; Cardoso, L. C.; Serrano, C. M.; de la Ossa, E. J. M.; Freire, C. S.; Vilela, C. Biobased films of nanocellulose and mango leaf extract for active food packaging: Supercritical impregnation versus solvent casting. *Food Hydrocolloids* **2021**, *117*, 106709.
(10) Moreira, J.; Vale, A. C.; Alves, N. M. Spin-coated freestanding films for biomedical applications. *Journal of materials chemistry B* **2021**, *9*, 3778-3799.
(11) Ponting, M.; Hiltner, A.; Baer, E. Polymer nanostructures by forced assembly: process, structure, and properties. *Macromolecular symposia* **2010**, *294*, 19-32.
(12) Li, Z.; Olah, A.; Baer, E. Micro-and nano-layered processing of new polymeric systems. *Progress in Polymer Science* **2020**, *102*, 101210.
(13) Ponting, M.; Burt, T. M.; Korley, L. T.; Andrews, J.; Hiltner, A.; Baer, E. Gradient multilayer films by forced assembly coextrusion. *Industrial & Engineering Chemistry Research* **2010**, *49*, 12111-12118.
(14) Song, H.; Singer, K.; Wu, Y.; Zhou, J.; Lott, J.; Andrews, J.; Hiltner, A.; Baer, E.; Weder, C.; Bunch, R. Layered polymeric optical systems using continuous coextrusion. *SPIE Proceeding*, *Nanophotonics and Macrophotonics for Space Environments III* **2009**, *7467*, 66-77.
(15) Xia, L.; Wu, H.; Guo, S.; Sun, X.; Liang, W. Enhanced sound insulation and mechanical properties of LDPE/mica composites through multilayered distribution and orientation of the mica. *Composites Part A: Applied Science and Manufacturing* **2016**, *81*, 225-233.
(16) Garofalo, E.; Scarfato, P.; Di Maio, L.; Incarnato, L. Tuning of co-extrusion processing conditions and film layout to optimize the performances of PA/PE multilayer nanocomposite films for food packaging. *Polymer Composites* **2018**, *39*, 3157-3167.

(17) Decker, J. J.; Meyers, K. P.; Paul, D. R.; Schiraldi, D. A.; Hiltner, A.; Nazarenko, S. Polyethylene-based nanocomposites containing organoclay: A new approach to enhance gas barrier via multilayer coextrusion and interdiffusion. *Polymer* **2015**, *61*, 42-54.
(18) Baer, E.; Zhu, L. 50th anniversary perspective: dielectric phenomena in polymers and multilayered dielectric films. *Macromolecules* **2017**, *50*, 2239-2256.
(19) Lamnawar, K.; Zhang, H.; Maazouz, A. Coextrusion of multilayer structures, interfacial phenomena. In *Encyclopedia of Polymer Science and Technology, 4th ed.; John Wiley & Sons Inc.: Hoboken, NJ, USA,* **2002***,* 36–38.
(20) Thellen, C.; Schirmer, S.; Ratto, J. A.; Finnigan, B.; Schmidt, D. Co-extrusion of multilayer poly (m-xylylene adipimide) nanocomposite films for high oxygen barrier packaging applications. *Journal of Membrane Science* **2009**, *340*, 45-51.
(21) Lu, B.; Bondon, A.; Touil, I.; Zhang, H.; Alcouffe, P.; Pruvost, S.; Liu, C.; Maazouz, A.; Lamnawar, K. Role of the Macromolecular Architecture of Copolymers at Layer–Layer Interfaces of Multilayered Polymer Films: A Combined Morphological and Rheological Investigation. *Industrial & Engineering Chemistry Research* **2020, *59*,** 22144–22154.
(22) Wang, J.; Adami, D.; Lu, B.; Liu, C.; Maazouz, A.; Lamnawar, K. Multiscale Structural Evolution and Its Relationship to Dielectric Properties of Micro-/Nano-Layer Coextruded PVDF-HFP/PC Films. *Polymers* **2020**, *12*, 2596.
(23) Boufarguine, M.; Guinault, A.; Miquelard-Garnier, G.; Sollogoub, C. PLA/PHBV films with improved mechanical and gas barrier properties. *Macromolecular Materials and Engineering* **2013**, *298*, 1065-1073.
(24) Lu, B.; Zhang, H.; Maazouz, A.; Lamnawar, K. Interfacial phenomena in multi-micro-/nanolayered polymer coextrusion: A review of fundamental and engineering aspects. *Polymers* **2021**, *13*, 417.
(25) Huang, R.; Silva, J.; Huntington, B.; Patz, J.; Andrade, R.; Harris, P.; Yin, K.; Cox, M.; Bonnecaze, R.; Maia, J. Co-Extrusion layer multiplication of rheologically mismatched polymers: a novel processing route. *International Polymer Processing* **2015**, *30*, 317-330.
(26) Han, C. D.; Shetty, R. Studies on multilayer film coextrusion I. The rheology of flat film coextrusion. *Polymer Engineering & Science* **1976**, *16*, 697-705.
(27) Han, C. D.; Shetty, R. Studies on multilayer film coextrusion II. Interfacial instability in flat film coextrusion. *Polymer Engineering & Science* **1978**, *18*, 180-186.
(28) Schrenk, W.; Alfrey Jr, T. Some physical properties of multilayered films. *Polymer Engineering & Science* **1969**, *9*, 393-399.
(29) Cheng, J.; You, X.; Cao, Z.; Wu, D.; Liu, C.; Pu, H. Effective Control of Laser-Induced Carbonization Using Low-Density Polyethylene/Polystyrene Multilayered Structure via Nanolayer Coextrusion. *Macromolecular Materials and Engineering* **2019**, *304*, 1800726.
(30) Cheng, J.-f.; Pu, H.-t. Orientation of LDPE crystals from microscale to nanoscale via microlayer or nanolayer coextrusion. *Chinese Journal of Polymer Science* **2016**, *34*, 1411-1422.
(31) Lin, X.; Fan, L.; Ren, D.; Jiao, Z.; Coates, P.; Yang, W. Enhanced dielectric properties of immiscible poly (vinylidene fluoride)/low density polyethylene blends by inducing multilayered and orientated structures. *Composites Part B: Engineering* **2017**, *114*, 58-68.
(32) Lamnawar, K.; Maazouz, A. Role of the interphase in the flow stability of reactive coextruded multilayer polymers. *Polymer Engineering & Science* **2009**, *49*, 727-739.
(33) Lamnawar, K.; Maazouz, A. Rheology and morphology of multilayer reactive polymers: effect of interfacial area in interdiffusion/reaction phenomena. *Rheologica Acta* **2008**, *47*, 383-397.
(34) Zhang, H.; Lamnawar, K.; Maazouz, A. Fundamental understanding and modeling of diffuse interphase properties and its role in interfacial flow stability of multilayer polymers. *Polymer Engineering & Science* **2015**, *55*, 771-791.

(35) Shin, E.; Hiltner, A.; Baer, E. The damage zone in microlayer composites of polycarbonate and styrene—acrylonitrile. *Journal of applied polymer science* **1993**, *47*, 245-267.
(36) Shin, E.; Hiltner, A.; Baer, E. The brittle-to-ductile transition in microlayer composites. *Journal of applied polymer science* **1993**, *47*, 269-288.
(37) Lai, C.-Y.; Hiltner, A.; Baer, E.; Korley, L. T. Deformation of confined poly (ethylene oxide) in multilayer films. *ACS applied materials & interfaces* **2012**, *4*, 2218-2227.
(38) Burt, T. M.; Jordan, A. M.; Korley, L. T. Investigating Interfacial Contributions on the Layer-Thickness-Dependent Mechanical Response of Confined Self-Assembly via Forced Assembly. *Macromolecular Chemistry and Physics* **2013**, *214*, 873-881.
(39) Messin, T.; Marais, S.; Follain, N.; Chappey, C.; Guinault, A.; Miquelard-Garnier, G.; Delpouve, N.; Gaucher, V.; Sollogoub, C. Impact of water and thermal induced crystallizations in a PC/MXD6 multilayer film on barrier properties. *European Polymer Journal* **2019**, *111*, 152-160.
(40) Cabrera, G.; Touil, I.; Masghouni, E.; Maazouz, A.; Lamnawar, K. Multi-Micro/Nanolayer Films Based on Polyolefins: New Approaches from Eco-Design to Recycling. *Polymers* **2021**, *13*, 413.
(41) Zhang, H.; Lamnawar, K.; Maazouz, A. Fundamental studies of interfacial rheology at multilayered model polymers for coextrusion process. In *AIP Conference Proceedings* **2015,** *1664*, 100008.
(42) Ree, M.; Kyu, T.; Stein, R. S. Quantitative small-angle light-scattering studies of the melting and crystallization of LLDPE/LDPE blends. *Journal of Polymer Science Part B: Polymer Physics* **1987**, *25*, 105-126.
(43) Siddaramaiah; Guruprasad, K.; Nagaralli, R.; Somashekarappa, H.; Guru Row, T.; Somashekar, R. Physicomechanical, optical, barrier, and wide angle X-ray scattering studies of filled low density polyethylene films. *Journal of applied polymer science* **2006**, *100*, 2781-2789.

Table of Contents